Joint International Topical Meeting on Mathematics & Computation and Supercomputing in Nuclear Applications (M&C + SNA 2007)
Monterey, California, April 15-19, 2007, on CD-ROM, American Nuclear Society, LaGrange Park, IL (2007)

SELF POINT DEFECTS CHARACTERISTICS AND THEIR DEPENDENCE ON $<11\bar{2}0>\{0001\}$ DISLOCATION STRESS FIELD IN α-Zr

D. A. Chulkin, V. M. Chernov and A. B. Sivak
A.A. Bochvar Institute of Inorganic Materials
123060, P.O. Box 369, Moscow, Russia
chernovv@bochvar.ru

ABSTRACT

In hcp Zr crystal, stable and metastable (including saddle point) configurations of self-point defects (SIA – self-intersitial atoms, vacancies) were found. Formation and migration energies, relaxation volumes and dipole tensors of these configurations were calculated by computer simulation methods with use the interaction potential developed in the framework of Finnis-Sinclair method. The stress fields of the straight edge dislocation $<11\bar{2}0>\{0001\}$ and spatial dependence of the interaction energy between these fields and self-point defects (SPD) were calculated in the frameworks of the anisotropic theory of elasticity. The dislocation stress fields significantly affect the point defects characteristics and behavior in hcp Zr.

Key Words: zirconium, self-point defects, dipole tensor, dislocation, anisotropic theory of elasticity, interaction energy.

1. INTRODUCTION

The zirconium alloys are widely used as the construction materials for active zones of nuclear reactors. Therefore the investigations of zirconium and its alloys microstructure are interesting in view of the development of new zirconium alloys.

Dislocations stress fields are the main source of the internal stresses in crystal. They crucially affect the self-point defect (SPD) kinetics, diffusion and absorption by dislocations [1]. These processes depend on the symmetry of the crystal lattice, the elastic anisotropy of the crystal and the crystal defect type. It is important to investigate the SPD characteristics and their dependence on the dislocation stress fields in hcp-Zr.

The interaction of impurities and dislocations in hcp crystals was investigated [2-5] by methods of the anisotropic theory of elasticity. The authors used the values of dipole tensors of impurities obtained from experiment. Since there is no experimental data on the SPD dipole tensors in Zr, in this paper they were found by means of computer simulation using the many-body interatomic potential. The spatial dependence of the interaction energy between the straight edge basal dislocation with Burgers vector $1/3<11\bar{2}0>$ stress field and SPD in stable and metastable (including saddle points) configurations were calculated in the frameworks of the anisotropic theory of elasticity.

2. SELF POINT DEFECTS CHARACTERISTICS CALCULATION METHOD

To calculate the characteristics of SPDs, the many-body potential [6] was chosen developed in the framework of Finnis-Sinclair method [7]. This potential describes the elastic properties of Zr well enough, gives almost correct *c*/*a* value (*c* and *a* are lattice constants). It predicts the basal migration of SIA as the most favorable, which indirectly follows from the experiment [8].

The computational cell is a hexagonal prism with hcp structure, consisting of three areas: the inner area I, the intermediate area II and external area III (Fig. 1). The atoms of the area I are moveable, and the atoms of the areas II, and III are fixed. The area III is necessary to nullify the forces acting upon the atoms of the area II in the perfect crystal.

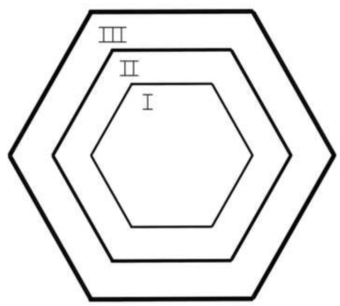

Figure 1. The schematic image of the computational cell, consisting of three areas: the inner area (I), the intermediate area (II), and the external area (III).

The equilibrium positions of the area I atoms were defined by means of the gradient descent method. The computational cell size guaranties that the boundary conditions affect defect characteristics no stronger than 0.5%. That goes if the area I atoms quantity is greater than 2000. The point defect makes the surrounding atoms to displace from their positions in the perfect crystal. Thus, the elastic dipole appears. It is characterized by the dipole tensor P_{ij} [9,10] (i, j=1, 2, 3 define the coordinate axes). The calculations of P_{ij} were performed according to [11]:

$$P_{ij} = \sum_n X_i^n F_j^n \tag{1}$$

where X_i^n are the Cartesian coordinates of the n-th atom, F_j^n are the projections of the forces acting upon the area II atoms from the area I atoms, which contain the relaxed defect. Eq. (1) contains the sum over the atoms of area II. The relaxation volumes of point defects were calculated as follows [12]:

$$V^R = S_{iikl} P_{kl} \tag{2}$$

here S_{ijkl} is the elastic compliance tensor of the crystal.

3. CHARACERISTICS OF SELF-POINT DEFECTS

Considered here SIA configurations are presented at Fig. 2, 3. Johnson-Beeler notation [13] of SIA configurations is accepted here: BC is the crowdion in the basal plane; BS is the basal split interstitial; C is the crowdion; S is the split interstitial, orthogonal to the basal plane; O is the octahedral interstitial; T is the tetrahedral interstitial; BO is the basal octahedral interstitial; BT is the basal tetrahedral interstitial, V is the vacancy. The formation energies E_F, the relaxation volumes V_R, the eigenvalues $P^{(s)}$ and the eigenvectors $\mathbf{e}^{(s)}$ (s = 1, 2, 3) of the dipole tensor, symmetry and the quantity N of crystallographic equivalent orientations of the considered stable, metastable (including saddle) SPD configurations in the absence of dislocation stress fields are given in Table I. The eigenvectors of dipole tensors are given in the Cartesian coordinate system: $\mathbf{e}_1 = [\bar{2}110]$, $\mathbf{e}_2 = [01\bar{1}0]$, $\mathbf{e}_3 = [0001]$.

Table I. The formation energy E^F (eV), the relaxation volume V^R (in atomic volumes), eigenvalues $P^{(s)}$ (eV) and eigenvectors $\mathbf{e}^{(s)}$ (s = 1, 2, 3) of the dipole tensor of concerned SPD configurations in hcp Zr. N is the quantity of crystallographic equivalent orientations of an elastic dipole.

SPD configuration	E_F	V_R	$P^{(1)}$	$P^{(2)}$	$P^{(3)}$	$\mathbf{e}^{(1)}$	$\mathbf{e}^{(2)}$	$\mathbf{e}^{(3)}$	N
BC	3.75	1.33	24.28	20.18	15.14	(1 0 0)	(0 1 0)	(0 0 1)	3
BS	3.77	1.35	24.47	20.38	15.48	(1 0 0)	(0 1 0)	(0 0 1)	3
C [1)]	3.98	1.28	13.80	17.77	26.44	(1 0 0)	(0 x y)	(0 -y x)	6
BO*	3.98	1.30	21.15	21.15	15.94	(1 0 0)	(0 1 0)	(0 0 1)	1
BT*	4.20	1.38	20.00	20.00	22.04	(1 0 0)	(0 1 0)	(0 0 1)	1
O*	4.13	1.50	19.00	19.00	30.10	(1 0 0)	(0 1 0)	(0 0 1)	1
T*	4.24	1.28	16.38	16.38	25.59	(1 0 0)	(0 1 0)	(0 0 1)	1
S	4.31	1.21	15.57	15.57	23.75	(1 0 0)	(0 1 0)	(0 0 1)	1
$\mathbf{SP^{BC}_{out}}$ [2)]	3.98	1.38	18.74	17.63	25.95	(1 0 0)	(0 x y)	(0 -y x)	6
$\mathbf{SP^{BC}_{in}}$ [3)]	3.98	1.31	19.03	21.80	18.21	(1 0 0)	(0 x y)	(0 -y x)	6
V	1.78	-0.27	-3.99	-3.99	-4.23	(1 0 0)	(0 1 0)	(0 0 1)	1
$\mathbf{SP^{V}_{in}}$	2.62	-0.28	-9.08	-0.66	-2.81	(1 0 0)	(0 1 0)	(0 0 1)	3
$\mathbf{SP^{V}_{out}}$ [4)]	2.67	-0.32	-9.23	1.32	-6.66	(1 0 0)	(0 x y)	(0 -y x)	6

* unstable

1) - 4) $y = \sqrt{1-x^2}$; 1) $x = 0.9965$; 2) $x = 0.9989$; 3) $x = 0.9403$; 4) $x = 0.8710$

SP is the saddle point.

The values of N equal to 1, 3, 6 correspond to the trigonal, the orthorhombic, and the monoclinic symmetries of point defects.

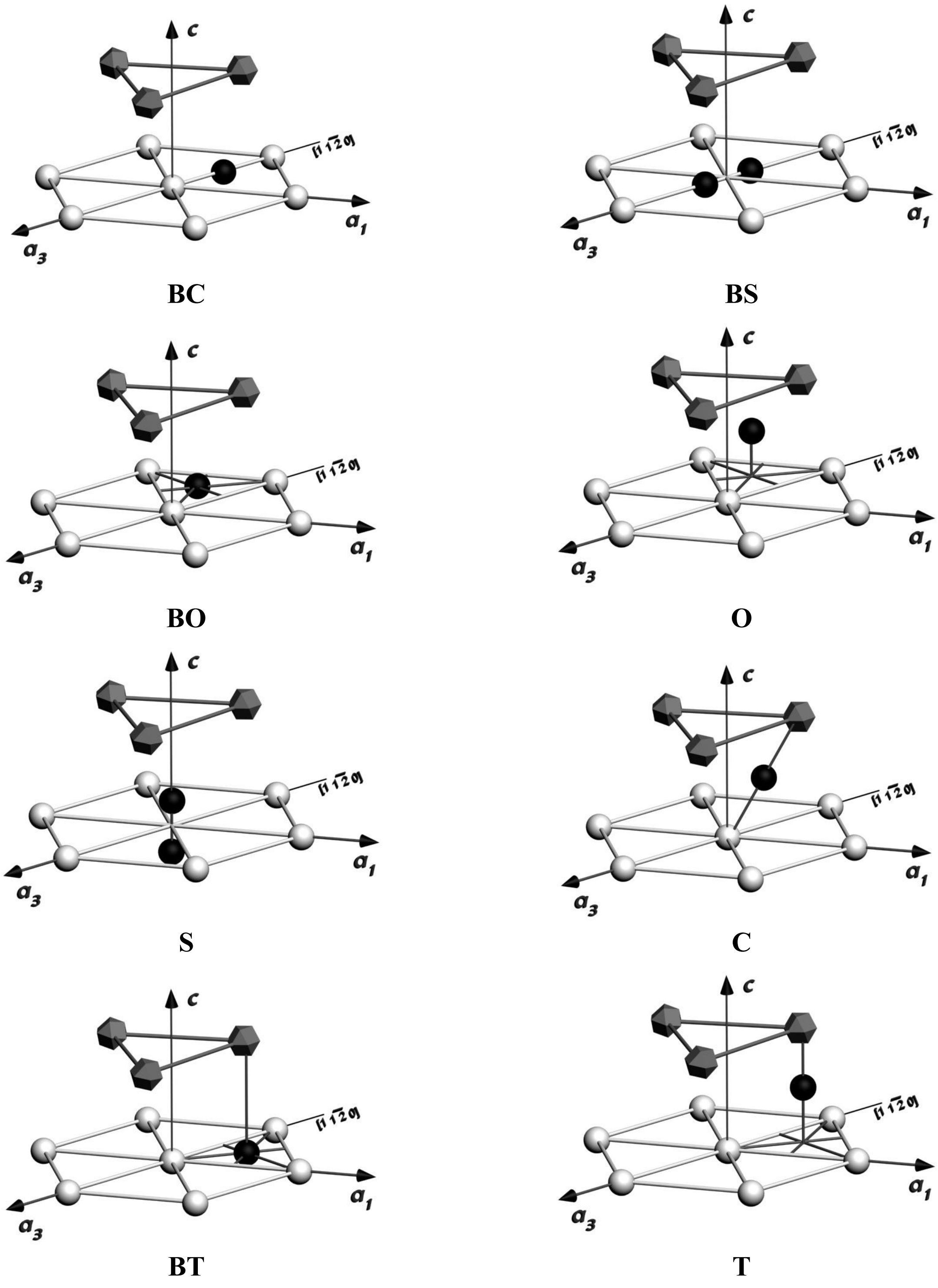

Figure 2. SIA configurations in hcp crystal lattice (*a_i*, *c* are the hexagonal coordinate system orts, *z* is the coordinate of axis along *c*).
– the first plane basal atoms, $z = 0$;
– the second plane basal atoms, $z = c$;
– SIA.

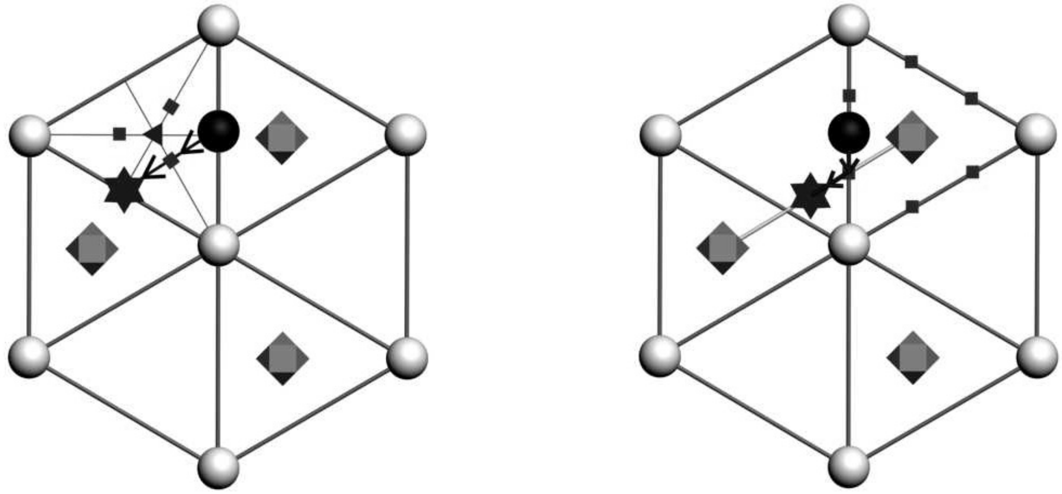

(a) (b)

Figure 3. BC saddle configurations:
(a) BC migrates in the basal plane with reorientation (SP^{BC}_{in});
(b) BC jumps out of the first basal plane to the second basal plane (SP^{BC}_{out}).
– the first plane basal atoms, $z = 0$;
– the second plane basal atoms, $z = c/2$;
– BO, $z = 0$;
– BC before jump, $z = 0$;
– BC after jump, $z = 0$; a) $z = 0$; b) $z = c/2$;
– the saddle point: a) $z = \pm 0.05c$; b) $z = c/4$.

Calculated here the formation energy and the relaxation volume coincide with the results [6] up to 0.01 eV and 0.01 Ω, correspondingly. The relaxations of the unstable configurations (T, BT, O, BO) were performed by fixing of SIA positions. In [6] it was obtained that BO configuration is stable.

The most energetically favorable configuration is the basal crowdion (BC) in the absence of dislocation stress fields. It has three equivalent orientations along the directions $[\bar{2}110]$, $[1\bar{2}10]$, and $[11\bar{2}0]$ (Table I).

The 1D migration mechanism of BC along the close-packed direction in the basal plane has the least energy barrier. The SIA moves from BC configuration to BS configuration, and then it moves to the next BC configuration with the initial orientation. The migration energy of this mechanism equals to 0.02 eV.

BC can migrate in the basal plane with reorientation with the migration energy 0.23 eV. This mechanism is depicted on Fig. 3a. All possible pairs of BC orientations before and after the migration in the basal plane and the notations of the corresponding saddle point orientations are given in Table II.

Table II. All possible pairs of BC orientations before and after the reorientation in the basal plane and the notations of the corresponding saddle points (SP) orientations.

Orientation before the migration	Orientation after the migration	SP notation
$[\bar{2}110]$	$[1\bar{2}10]$	A± *
$[\bar{2}110]$	$[11\bar{2}0]$	B±
$[11\bar{2}0]$	$[1\bar{2}10]$	C±
* The signs «+» and «–» correspond to saddle points situated on different sides of the basal plane ($z = \pm\, 0.05c$).		

To migrate from one basal plane to another, the SIA has to pass through one of the saddle points, depicted on Fig. 3b. These saddle points are situated between the basal planes at the height of $z = c/4$. BC needs to overcome the 0.23 eV energetic barrier to migrate out of the basal plane. All possible pairs of BC orientations before and after the migration from the basal plane $z = 0$ to another basal plane $z = c/2$ and the notations of the corresponding saddle points orientations are given in Table III.

The vacancy migration energies in and out of the basal plane are 0.84 eV and 0.89 eV, correspondingly.

Table III. All possible pairs of BC orientations before and after migration out of the basal plane and notations of corresponding saddle points (SP) orientations.

Orientation before migration ($z = 0$)	Orientation after the migration ($z = \pm\, c/2$)	SP notation
$[11\bar{2}0]$	$[\bar{2}110]$	A± *
$[\bar{2}110]$	$[11\bar{2}0]$	
$[11\bar{2}0]$	$[1\bar{2}10]$	B±
$[1\bar{2}10]$	$[11\bar{2}0]$	
$[1\bar{2}10]$	$[\bar{2}110]$	C±
$[\bar{2}110]$	$[1\bar{2}10]$	
* The signs «+» and «–» correspond to saddle points situated on different sides of the basal plane ($z = \pm\, c/4$).		

4. INTERACTION OF DISLOCATIONS AND POINT DEFECTS

The stress field σ_{ij} ($i, j = 1, 2, 3$) of the straight edge dislocation in the slip system $[11\bar{2}0](0001)$ with Burgers vector $\frac{1}{3}[11\bar{2}0]$ was calculated in the frameworks of the anisotropic theory of elasticity [14]. These calculations were performed using the elastic constants of hcp Zr specified by the interatomic potential [6] chosen for defect characterisitics calculations. C_{11}= 150 GPa, C_{12} = 85 GPa, C_{13} = 67 GPa, C_{33} = 175 GPa, and C_{44} = 36 GPa.

The formation energy of a point defect E_d^F may vary due to the interaction with the dislocation elastic stress field:

$$E_d^F = E^F + E_{\text{int}}(\mathbf{r}). \tag{4}$$

Here E_F is the formation energy of the point defect in the presence of the dislocation, **r** is the radius-vector of the point defect relative to the dislocation.

The interaction energy between the dislocation and the point defect can be represented as follows [9,10,15]:

$$E_{\text{int}}(\mathbf{r}) = -P_{ij}\varepsilon_{ij}^d(\mathbf{r}) = E_0\frac{b}{r}f(\phi), \quad \int_0^{2\pi}[f(\phi)]^2 d\phi = \pi, \tag{5}$$

where r and ϕ are the polar coordinates of the point defect, the polar coordinate system is chosen so that the dislocation core is situated in its origin and the angle ϕ is counted off from the dislocation slip plane; ε_{ij}^d is the dislocation elastic strain tensor; $f(\phi)$ is the function defining the angular dependence of the interaction energy; E_0 is the binding energy of the dislocation and the point defect; b is the magnitude of the dislocation Burgers vector.

Dislocation stress field eliminates degeneracy of the formation energies of crystallographically equivalent orientations of SPDs. The binding energies E_0 calculated according to Eq. (5) for all considered configurations and orientations of SPD are listed in Table IV. As one can see from Table IV, the magnitude of the interaction energy E_0 essentially depends on the configuration and the orientation of SPD.

Taking into account Eq. (4), one can determine the most energetically favorable SIA configurations in the whole space around the dislocation (Fig. 4). The calculations reveal that the most energetically favorable SIA configuration above the dislocation slip plane is oriented along the direction $[11\bar{2}0]$ BC configuration, parallel to the dislocation Burgers vector (except for a small area in the vicinity of the dislocation where O configuration is stable). Two minima of this configuration formation energy in a given basal plane are situated at the rays ϕ = 72.3° and ϕ = 107.7°, and the local maximum is situated at the ray ϕ = 90°. Below the slip plane, there is an area with the stable C configuration.

If the point defect is located outside of the dislocation slip plane, it has to jump out of one basal plane to another in order to approach to the $[11\bar{2}0](0001)$ edge dislocation core. The most favorable SIA configuration in the presence of this dislocation is BC with $[11\bar{2}0]$ orientation. As one can see from Table III, after the jump to the neighboring basal plane, BC finds itself in one of the unfavorable orientations ($[\bar{2}110]$ or $[1\bar{2}10]$). After that BC is able to jump to the next basal plane to the energetically favorable $[11\bar{2}0]$ orientation, or to reorient to this orientation in the same plane. Calculations show that the second process has lower energy barrier. When the distance to the dislocation decreases, this barrier increases in the area of the minimal SIA formation energy ($\phi = 72.3°$ and $\phi = 107.7°$) (Fig. 5(a)). On the contrary, the energetic barrier of the vacancy migration to the dislocation in the area of the minimal vacancy formation energy ($\phi = 270°$) increases with the distance to the dislocation core (Fig. 5(b)).

Table IV. The binding energy E_0 (eV) of the edge dislocation $[11\bar{2}0](0001)$ and SPD in Zr.

SPD configuration	Orientation	E_0	SPD configuration	Orientation	E_0
BC	$[11\bar{2}0]$	2.315	$\mathbf{SP^{BC}_{in}}$ *	A±	1.669
	$[\bar{2}110]$	2.008		B±	1.844
	$[1\bar{2}10]$	2.008		C±	1.852
BS	$[11\bar{2}0]$	2.324	$\mathbf{SP^{BC}_{out}}$	A±	1.493
	$[1\bar{2}10]$	2.017		B±	1.493
	$[\bar{2}110]$	2.017		C±	1.558
C	$[20\bar{2}3]$, $[20\bar{2}\bar{3}]$	1.422	**V**	$[0001]$	0.342
	$[0\bar{2}23]$, $[20\bar{2}\bar{3}]$	1.422	$\mathbf{SP^{V}_{in}}$	$[11\bar{2}0]$	0.905
	$[\bar{2}203]$, $[\bar{2}20\bar{3}]$	1.226		$[\bar{2}110]$	0.267
BO	$[0001]$	1.961		$[1\bar{2}10]$	0.267
BT	$[0001]$	1.701	$\mathbf{SP^{V}_{out}}$	$[20\bar{2}3]$, $[20\bar{2}\bar{3}]$	0.508
O	$[0001]$	1.606		$[0\bar{2}23]$, $[20\bar{2}\bar{3}]$	0.508
T	$[0001]$	1.373		$[\bar{2}203]$, $[\bar{2}20\bar{3}]$	0.857
S	$[0001]$	1.303			

*SP is the saddle point.

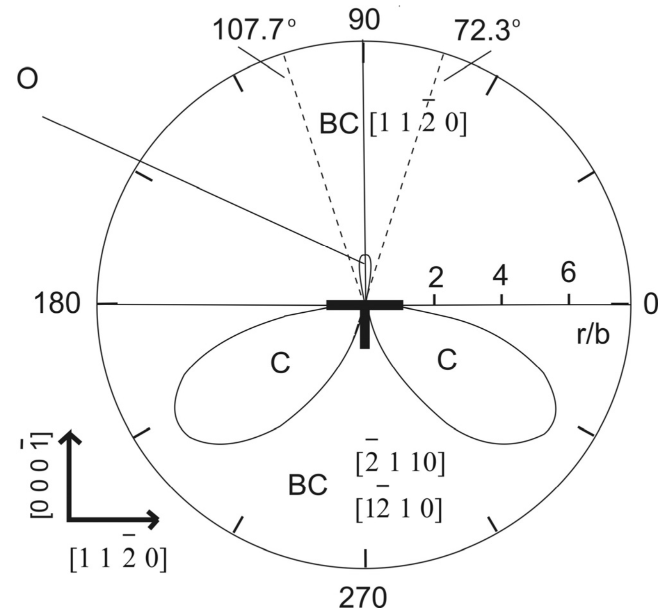

Figure 4. Stabilization regions of different SIA configurations. Dotted lines are the rays, at which the BC $[11\bar{2}0]$ formation energy is minimal under the migration in the given basal plane.

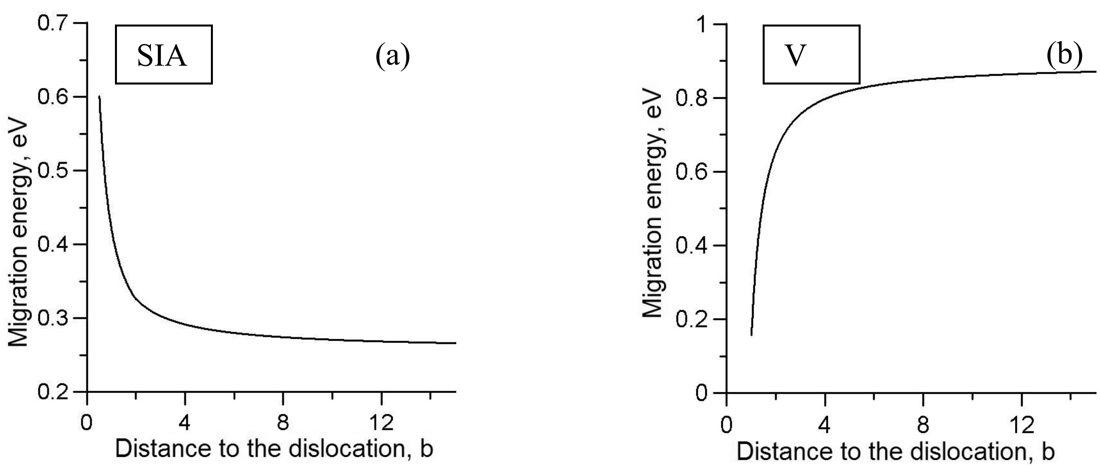

Figure 5. The migration energy of an SPD located to the dislocation vs. distance to the dislocation curve. SPD is located at the ray ϕ = const of its minimal formation energy: (a) SIA, ϕ = 72.3° and 107.7°; (b) V, ϕ = 270°.

5. CONCLUSIONS

The formation and migration energies, the relaxation volume and the dipole tensor of stable and metastable (including saddle) configurations of self-point defects (SIA – self-intersitial atoms, vacancies) were calculated by molecular statics with use of the interaction potential developed in the framework of Finnis-Sinclair method. The most energetically favorable configuration is the basal crowdion (BC) in the absence of the dislocation stress fields. It possesses three equivalent orientations along the closed package directions $[\bar{2}110]$, $[1\bar{2}10]$, and $[11\bar{2}0]$.

The stress field of the straight edge dislocation in the slip system $[11\bar{2}0](0001)$ and the spatial dependences of the interaction energy between this field and self-point defects were calculated in the framework of the anisotropic theory of elasticity.

The most favorable SIA configuration in the attraction area is BC oriented along the Burgers vector. Two minima of this configuration formation energy in a given basal plane are located at the rays that make up the angles $\phi = 72.3°$ and $\phi = 107.7°$ with the slip plane, and the local maximum is located at $\phi = 90°$. The vacancy formation energy in a given basal plane is minimal at $\phi = 270°$.

In order to approach to the edge dislocation, a SIA and a vacancy have to jump out of one basal plane to another. As the distance to dislocation decreases, the corresponding migration energy increases for the SIA and decreases for the vacancy in the mentioned above areas of minimal formation energy of the stable SIA configuration and vacancy.

ACKNOWLEDGMENTS

The present work was funded by Russian Foundation for Basic Research (project RFBR 05-02-08128ofi-e).

REFERENCES

1. V. L. Indenbom, J. Lothe, *Elastic strain fields and dislocation mobility*, North-Holland, Amsterdam (1992).
2. V. M. Chernov, M. M. Savin, “Elastic Interacrion of Dislocations with Tetragonal Point Defects in Anisotropic H.C.P. Cystals,” *Phys. Stat. Sol.*, **38,** pp. 761-768 (1976).
3. C. K. Syn, A. Ahmadieh, J. W. Morris, “Elastic solute-dislocation interaction in an anisotropic hcp crystal,” *Philos. Mag.*, **31**, pp.883-891 (1975).
4. M. M. Savin,V. M. Chernov, “Elastic Interacrion of Dislocations with Orthorhombic and $[001]$-Monoclinic Point Defects in H.C.P. Crystals,” *Crystallografiya*, **28** pp.115-122 (1983).
5. M. M. Savin,V. M. Chernov, “Elastic Interaction of Dislocations with $<001>$-Monoclinic Point Defects in H.C.P. Crystals,” *Crystallografiya*, **28** pp.642-646 (1983).
6. G. J. Ackland, S. J. Wooding, D. J. Bacon, “Defect, surface and displacement-threshold properties of α - zirconium simulated with a many-body potential,” *Philos. Mag. A*, **71**, pp.553 - 565 (1995).

7. M. W. Finnis, J. E. Sinclair, "A simple empirical N-body potential for transition metals," *Philos. Mag. A*, **50**, pp. 45 - 55 (1984).
8. C. H. Woo, "Rate theory analysis of radiation damage effects near surfaces in hexagonal metals," *Philos. Mag. A*, **63**, pp.915 – 923 (1991).
9. J. D. Eshelby, "*The Continuum Theory of Lattice Defects*," *Solid State Physics*, **3**, pp.79-144 (1956).
10. E. Kröner, *Kontinuumstheorie der Versetzungen und Eigenspannungen*, Springer, Berlin – Göttingen – Heidelberg (1958).
11. H. R. Schober, K. W. Ingle, "Calculation of Relaxation Volumes, Dipole Tensors and Kanzaki Forces for Point Defects" *J. Phys. F: Metal Phys.*, **10**, pp.575-581 (1980)
12. G. Leibfrid, N. Brouer, *Point Defects in Metals,* Springer-Verlag, Berlin, 1978
13. R. A. Johnson, J. R. Beeler, *Interatomic Potentials and Crystalline Defects*, AIME, New York, USA (1981)
14. J. P. Hirth, J. Lothe, *Theory of Dislocations*, John Wiley & sons, New York (1982).
15. V. V. Ivanov, V. M. Chernov, "Influence of Dislocation Field on Stable Configurations of Self-Interstitials in Cubic Metals," *Atomnaya Energiya*, **61**, pp.422-431 (1986).